

# Reactive Collisions of Hyperthermal Ions with Oxide Surfaces

M. Maazouz, C. L. Quinteros, T. Tzvetkov, P. L. Maazouz, X. Qin, T. L. O. Barstis,<sup>\*</sup> and D. C. Jacobs

*Dept. of Chemistry and Biochemistry, University of Notre Dame, Notre Dame, IN 46556*

**Abstract.** Hyperthermal energy ions ( $\text{NO}^+$  and  $\text{O}^+$ ) are reacted with thin oxide films grown on Al(111) and Si(100), respectively. The scattered ionic products ( $\text{NO}_2^-$  and  $\text{O}_2^-$ , respectively) are detected with mass-, energy-, and angular-resolution. The translational energy distributions of the products are correlated with the collision energy, suggesting that the abstraction product emerges from the surface before it, or the incident ion, has had time to equilibrate. Thresholds for O-atom abstraction are 9 eV for  $\text{NO}^+$  incident on O/Al(111) and 16 eV for  $\text{O}^+$  on  $\text{SiO}_x$ . The data support an Eley-Rideal mechanism, in which the incident ion neutralizes along the inbound trajectory, abstracts an adsorbed oxygen atom through a direct collision, and scatters from the surface as a molecular anion.

## INTRODUCTION

Hyperthermal energy ion/surface collisions can activate a number of reactive processes, e.g., electron transfer, fragmentation, atom abstraction, oxidation, and implantation. Scattering experiments on well-characterized surfaces offer an advantageous perspective for elucidating reaction mechanisms; ion beams allow one to measure how an incident ion's energy and approach geometry affect its reaction probability with the surface target. In the hyperthermal energy regime ( $10^0 - 10^2$  eV), chemical barriers are easily surmounted without significant damage to the surface.

Surface reaction mechanisms are often categorized as falling into one of two limiting cases: Langmuir-Hinshelwood (LH) or Eley-Rideal (ER).<sup>1</sup> In the LH mechanism, both reactants are thermally equilibrated with the surface prior to reaction. In the ER mechanism, an incident gaseous particle reacts directly with a surface adsorbate without first trapping on the surface. In reality, a continuum exists between these two cases, and hot-atom precursors have been implicated for a variety of systems.<sup>2</sup> Deciphering the

precise mechanism of a reaction requires a thorough study of the corresponding reaction dynamics.<sup>3</sup>

Two systems are presented here in which the incident ion abstracts an oxygen atom from a surface oxide layer.<sup>4,5</sup> The interaction of hyperthermal energy  $\text{O}^+$  with  $\text{SiO}_x$  is relevant to the low-earth orbit environment, where energetic oxygen atoms and ions continuously bombard protective coatings such as  $\text{SiO}_2$  on orbiting spacecraft.<sup>6</sup> Furthermore, oxygen plasma processing in the microelectronics industry is frequently used to etch and to deposit oxide films on silicon.<sup>7</sup> Despite these important technological applications, a fundamental understanding of how hyperthermal energy  $\text{O}^+$  reacts with silicon oxide is lacking.

Many investigators have observed that hyperthermal molecular ions can abstract adsorbed species (predominantly hydrogen) from a surface; yet, the precise mechanism of such reactions is not definitively assigned.<sup>8</sup> Using state-selected  $\text{NO}^+(\text{X}^1+)$  ions, the abstraction dynamics on O/Al(111) are studied with precise control over the initial conditions of the reaction.

<sup>\*</sup> Present address: Department of Chemistry and Physics, St. Mary's College, Notre Dame, IN 46556.

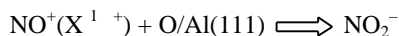
## EXPERIMENTAL

The oxide surfaces are prepared *in situ* within an ultrahigh vacuum scattering chamber. Prior to introducing the  $\text{NO}^+$  ions, the Al(111) surface is dosed with 750 L  $\text{O}_2$  through a leak valve.<sup>4</sup> This results in a thin film containing chemisorbed and oxide phases.<sup>9</sup> An oxide layer is grown on Si(100) through 30 eV  $\text{O}^+$  ion bombardment.<sup>5</sup> Prolonged exposure to the ion beam does not result in a thicker oxide film, because the incident oxygen ions erode the film at the same rate as oxygen deposition.<sup>10</sup>

A monoenergetic, mass-selected ion beam is targeted at each of the oxidized surfaces. The  $\text{O}^+(^4\text{S})$  ions are formed in a Colutron plasma source;<sup>5</sup> whereas the  $\text{NO}^+(\text{X}^1\text{ }^+)$  ions are created in a state-specific manner at the intersection of a pulsed molecular beam and the frequency-doubled output of a Nd:YAG-pumped dye laser.<sup>4</sup> Scattered ionic products are detected with mass-, energy-, and angular-resolution.

## RESULTS AND DISCUSSION

The abstraction of oxygen atoms from oxide surfaces is illustrated through two model reactions:



Following a discussion of the results for each reaction, the scattering dynamics for the two systems will be compared.

### $\text{NO}^+(\text{X}^1\text{ }^+)$ on O/Al(111)

Figure 1 presents the  $\text{NO}_2^-$  yield as a function of  $\text{NO}^+(\text{X}^1\text{ }^+)$  collision energy for a Al(111) surface dosed with 750 L  $\text{O}_2$ . The  $\text{NO}_2^-$  yield exhibits a threshold energy,  $9 \pm 1$  eV, above which the yield increases monotonically with  $\text{NO}^+$  translational energy. The observed threshold is consistent with thermodynamic estimates of the reaction barrier.<sup>4</sup> The  $\text{NO}_2^-$  yield also scales with the total coverage of oxygen pre-dosed on the surface.

If a LH mechanism were operative, the incident NO would thermally equilibrate with the surface prior to forming  $\text{NO}_2$ . However, the velocity distribution of scattered  $\text{NO}_2^-$  is nonthermal and cannot be described by a Maxwell-Boltzmann distribution at the surface

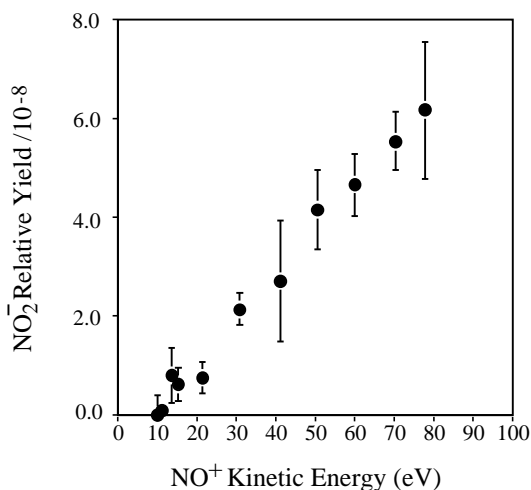


**FIGURE 1.** The collision-energy dependence to  $\text{NO}_2^-$  emergence (From Ref. 4). The Al(111) surface was dosed with 750 L  $\text{O}_2$  prior to  $\text{NO}^+$  scattering at normal incidence.

temperature (See Fig. 2). Moreover, the mean translational energy of scattered  $\text{NO}_2^-$  increases with  $\text{NO}^+$  collision energy. This correlation implies that the reaction occurs via a direct collision between an incident NO molecule and an adsorbed oxygen atom. The data indicate that neither the incident NO molecule nor the scattered  $\text{NO}_2^-$  product resides on the surface long enough to become thermally accommodated. It is proposed that  $\text{NO}_2^-$  is

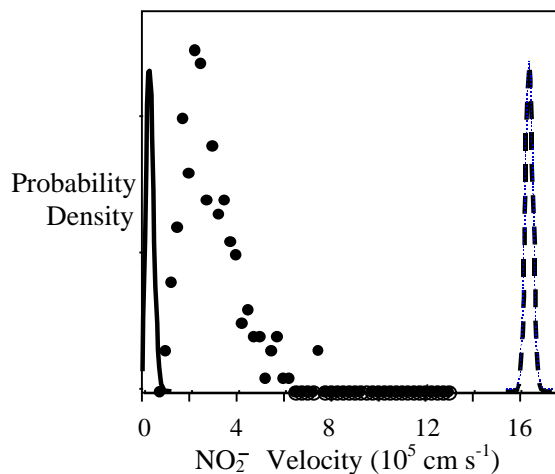
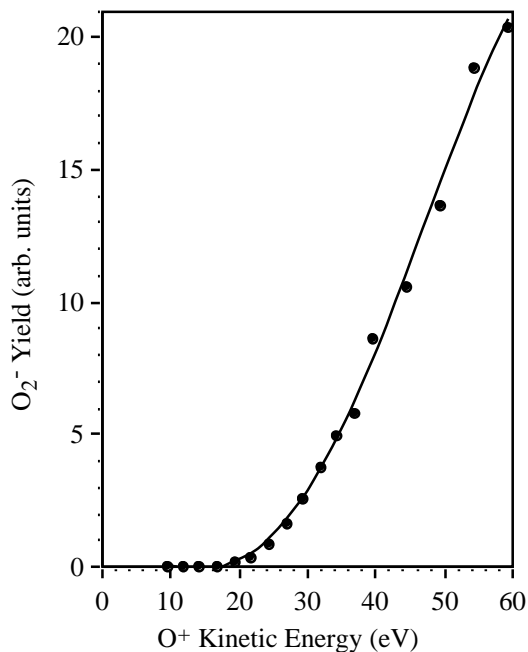


**Figure 2.** Velocity distribution of  $\text{NO}_2^-$  produced from 40 eV  $\text{NO}^+$  abstracting an oxygen atom from O/Al(111). For comparison, the plot shows the velocity distribution (dashed line) of incident  $\text{NO}^+$ , and the predicted Maxwell-Boltzmann distribution (solid curve) if  $\text{NO}_2^-$  were thermally equilibrated with the surface at 300 K.

formed by a three-step mechanism: incident  $\text{NO}^+$  is neutralized close to the surface; nascent NO impacts an adsorbed oxygen atom; and  $\text{O}^-$  is abstracted by NO to form  $\text{NO}_2^-$  via an ER mechanism.<sup>4</sup>

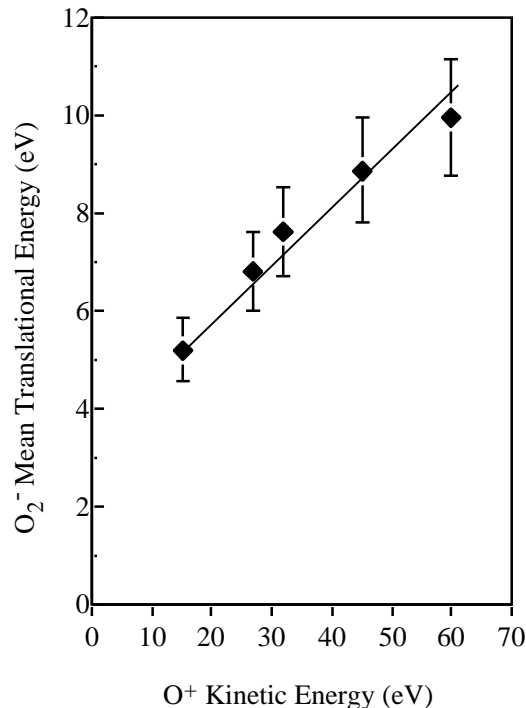
### $\text{O}^+$ on Oxidized Si(100)

Figure 3 shows the collision-energy dependence to the  $\text{O}_2^-$  yield for  $\text{O}^+$  scattering on a  $\text{SiO}_x$  surface. The threshold for  $\text{O}_2^-$  emergence occurs at  $16 \pm 1$  eV.<sup>5</sup> Isotopic labeling experiments have helped to define the origin of each oxygen atom in the  $\text{O}_2^-$  product. An isotopically pure  $\text{Si}^{16}\text{O}_x$  film was grown using a mass-selected  $^{16}\text{O}^+$  beam. After a  $^{16}\text{O}^+$  dose of  $1 \times 10^{16}$  ions/cm<sup>2</sup>, scattering commenced with a mass-selected  $^{18}\text{O}^+$  beam. For all  $^{18}\text{O}^+$  incident energies (up to 60 eV) and scattering angles studied ( $45^\circ$ - $135^\circ$ ),  $> 96\%$  of the scattered  $\text{O}_2^-$  appeared at a mass equal to 34 u. Therefore,  $\text{O}_2^-$  is produced when one oxygen atom from the incident ion beam ( $^{18}\text{O}$ ) combines with one oxygen atom from the silicon oxide layer ( $^{16}\text{O}$ ). The lack of signal corresponding to  $^{32}\text{O}_2^-$  and  $^{36}\text{O}_2^-$  precludes physical sputtering and projectile recombination, respectively, as significantly contributing to  $\text{O}_2^-$  formation.



**FIGURE 3.**  $\text{O}_2^-$  yield as a function of  $\text{O}^+$  collision energy.  $\text{O}^+$  is incident at  $45^\circ$  on an oxidized Si(100) surface (From Ref. 5). The appearance threshold for  $\text{O}_2^-$  is  $16 \pm 1$  eV. The curve is drawn to guide the eye.

A variety of remaining mechanisms can describe the association of a projectile and a surface oxygen atom to form  $\text{O}_2^-$ ; yet most can be eliminated in consideration of the experimental evidence. In a LH mechanism, the  $\text{O}_2^-$  product would be expected to emerge with a translational energy distribution that is independent of the collision energy. However, Fig. 4 shows that the mean kinetic energy of scattered  $\text{O}_2^-$  correlates strongly with the incident  $\text{O}^+$  kinetic energy. Therefore, the projectile ( $^{18}\text{O}$ ) must be reacting before it has a chance to thermally equilibrate with the surface. Furthermore, the product  $\text{O}_2^-$  angular distribution is peaked near the specular angle and shows a correlation with the incident  $\text{O}^+$  angle.<sup>11</sup> This is direct evidence for an abstraction reaction occurring in a single collision event (ER mechanism). If the  $\text{O}^+$  ion were to undergo multiple bounces on the corrugated surface before abstracting the adsorbed oxygen atom, then the incident particle would lose memory of its initial direction, and the product angular distribution would be independent of the incident angle. It is conceivable however, that an angular correlation could persist if the incident oxygen atom underwent a single collision with the substrate and immediately abstracted an adsorbed oxygen atom on the outgoing trajectory.



**FIGURE 4.** Mean translational energy of scattered  $\text{O}_2^-$  product versus  $\text{O}^+$  kinetic energy (From Ref. 5).  $\text{O}^+$  is incident at  $45^\circ$  on an oxidized Si(100) surface.

## Comparison of Results

The two systems display a similar threshold behavior for abstraction. While the energetics for the two reactions are comparable, it is worth noting that the scattering of  $\text{NO}^+$  on O/Al(111) was performed at normal incidence, while  $\text{O}^+$  was incident on  $\text{SiO}_x$  at  $45^\circ$ . Correspondingly, the former system exhibited a lower threshold than the latter.

In both systems, the mean translational energy of the product,  $\langle E_{\text{prod}} \rangle$ , shows a linear dependence on the collision energy,  $E_{\text{coll}}$ . A simple relation between the two quantities can be parameterized as:

$$\langle E_{\text{prod}} \rangle = F (E_{\text{collision}} - E_{\text{threshold}}) + E_o \quad (1)$$

where  $E_{\text{threshold}}$  is the collision energy at which abstraction products first emerge,  $E_o$  is the mean translational energy of the products at threshold, and  $F$  is the fraction of excess incident energy that appears as translational energy in the products. Table 1 lists the values of these parameters for the two systems. At every incident energy,  $\text{O}_2^-$  emerged with greater kinetic energy than did  $\text{NO}_2^-$ . This may be attributed to three different effects. First, the scattering angle was  $\sim 90^\circ$  and  $180^\circ$  in the two experiments, respectively. Second, the departing  $\text{NO}_2^-$  molecule is more massive than  $\text{O}_2^-$ . Binary collision theory would predict that both of these effects favor  $\text{O}_2^-$  as having the larger kinetic energy. Third, the final energy release is distributed into more degrees of freedom within the larger molecule. Consequently,  $\text{NO}_2^-$  should emerge with less translational energy and more internal energy than its  $\text{O}_2^-$  counterpart.

**TABLE 1. Energetics of Abstraction**

System	$E_{\text{threshold}}$ (eV)	$E_o$ (eV)	$F$
$\text{NO}^+ + \text{O}/\text{Al}(111)$	9	1.1	0.023
$\text{O}^+ + \text{SiO}_x$	16	5.1	0.12

The two systems described here represent the first demonstration that hyperthermal ions can directly abstract oxygen atoms from an oxide surface. In both cases, the scattering dynamics strongly suggest that the oxygen atom is abstracted through an Eley-Rideal mechanism.

## ACKNOWLEDGMENTS

Support from the National Science Foundation (CHE-9986374 and CHE96-15878) and the Air Force Office of Scientific Research (F49620-98-1-0029) are gratefully acknowledged.

## REFERENCES

- Weinberg, W. H., "Kinetics of Surface Reactions" in *Advances in Gas-Phase Photochemistry and Kinetics: Dynamics of Gas-Surface Interactions*, edited by C. T. Rettner and M. N. R. Ashfold, London: Royal Society of Chemistry, 1991, pp. 171 - 219.
- Kratzer, P., *J. Chem. Phys.* **106**, 6752 – 6763 (1997).
- Rettner, C. T. and Auerbach, D. J., *Science* **263**, 365 - 367 (1994).
- Maazouz, M., Barstis, T. L. O., Maazouz, P. L., and Jacobs, D. C., *Phys. Rev. Letters* **84**, 1331 - 1334 (2000).
- Quinteros, C. L., Tzvetkov, T., and Jacobs, D. C., *J. Chem. Phys.*, **113**, 5119 - 5122 (2000).
- Murad, E., *Annu. Rev. Phys. Chem.* **49**, 73 - 98 (1998).
- Herbots, N., Hellman, O. C., Ye, P., Wang, X., and Vancauwenberghe, O., "Chemical Reactions During Thin Film Synthesis By Low Energy Ions: Ion Beam Oxidation (IBO) and Ion Beam Nitridation (IBN)" in *Low Energy Ion-Surface Interactions*, edited by J. W. Rabalais, New York: John Wiley & Sons, 1994, pp. 387 - 480.
- Wu, Q. and Hanley, L., *J. Phys. Chem.* **97**, 2677 - 6459 (1993).
- Brune, H., Wintterlin, J., Trost, J., Ertl, G., Wiechers, J., and Behm, R. J., *J. Chem. Phys.* **99**, 2128 – 2148 (1993).
- Todorov, S. S. and Fossum, E. R., *J. Vac. Sci. Technol. B* **6**, 466-469 (1988).
- Quinteros, C. L., Tzvetkov, T., Qin, X., and Jacobs, D. C., (unpublished).